

# Hemodynamic Effects of Anti-Vascular Endothelial Growth Factor Injections on Optical Coherence Tomography Angiography in Diabetic Macular Edema Eyes

Jessica Song<sup>1</sup>, Bonnie B. Huang<sup>1</sup>, Janice X. Ong<sup>1</sup>, Nicholas Konopek<sup>1</sup>, and Amani A. Fawzi<sup>1</sup>

<sup>1</sup> Department of Ophthalmology, Feinberg School of Medicine, Northwestern University, Chicago, Illinois, USA

**Correspondence:** Amani A. Fawzi, 645 N Michigan Suite 440, Chicago, IL 60611, USA.  
e-mail: [afawzimd@gmail.com](mailto:afawzimd@gmail.com)

**Received:** April 13, 2022

**Accepted:** July 21, 2022

**Published:** October 3, 2022

**Keywords:** diabetic macular edema; anti-VEGF injection; OCTA

**Citation:** Song J, Huang BB, Ong JX, Konopek N, Fawzi AA. Hemodynamic effects of anti-vascular endothelial growth factor injections on optical coherence tomography angiography in diabetic macular edema eyes. *Transl Vis Sci Technol.* 2022;11(10):5. <https://doi.org/10.1167/tvst.11.10.5>

**Purpose:** To evaluate retinal hemodynamic responses to anti-vascular endothelial growth factor (VEGF) injection in eyes with diabetic macular edema using optical coherence tomography angiography (OCTA). We performed a comparison of two different thresholding methods to identify the most accurate for studying the vessel density (VD) in diabetic macular edema eyes.

**Methods:** The study prospectively included 26 eyes of 22 subjects (aged  $60.2 \pm 13.7$  years) who underwent OCTA scan before and after anti-VEGF injection (mean interval between OCTA =  $31.1 \pm 17.3$  days). We analyzed adjusted flow index, VD, and Skeletonized vessel length density in the parafoveal area (3-mm annulus with a 1-mm inner circle), along with full-thickness fovea avascular zone area and central foveal thickness (CFT). Using averaged scans VD as the ground truth, we compared two different algorithms for VD at the different plexuses. Longitudinal changes were assessed using a generalized linear model correcting for central foveal thickness and Q-score.

**Results:** We found significantly decreased adjusted flow index in the DCP layer ( $P = 0.010$ ) at the follow-up. Furthermore, foveal avascular zone ( $P < 0.001$ ) and central foveal thickness ( $P = 0.003$ ) showed significant decrease on follow-up compared with baseline. Comparing the thresholding algorithms showed that vessel length density-based thresholding was more accurate for quantifying the DCP VD.

**Conclusions:** The adjusted flow index decreased significantly in the DCP layer on follow-up OCTA scan, suggesting vascular flow disruption and decreased deep retinal perfusion after anti-VEGF injection. Our results also highlight the fact that the choice of thresholding method is particularly critical for DCP quantification in eyes with diabetic macular edema.

**Translational Relevance:** Findings confirmed impaired deep retinal capillary flow after anti-VEGF injection.

## Introduction

Diabetic macular edema (DME) is a leading cause of visual loss among diabetics, with a prevalence approaching 30% depending on diabetic retinopathy (DR) severity, type of diabetes, and duration of the disease.<sup>1</sup> The pathophysiology of DME is complex but upregulation of vascular endothelial factor (VEGF) leading to breakdown of the inner blood-retina barrier with retinal vascular leakage is thought to

be a major contributing factor.<sup>2</sup> Anti-VEGF therapy has, therefore, become the first-line treatment for DME.<sup>3</sup>

In addition to their role in DME treatment, anti-VEGF injections have become the new gold standard for a considerable variety of other retinal diseases.<sup>4</sup> Although the clinical outcomes of anti-VEGF therapy have generally been positive, several reports have raised potential concerns regarding anti-VEGF effects on retinal hemodynamics. In eyes with neovascular age-related macular degeneration, progressive retinal

arteriolar vasoconstriction was associated with each subsequent intravitreal anti-VEGF injection as seen on retinal vessel analyzer.<sup>5</sup> This finding was replicated in 27 eyes with branch retinal vein occlusion, where significant vasoconstriction was observed in the large retrobulbar retinal arteries along with a decrease in flow velocities measured on color Doppler imaging.<sup>6</sup> Furthermore, sustained retinal arteriolar vasoconstriction was seen 1 year after the first intravitreal anti-VEGF injection in eyes with neovascular age-related macular degeneration.<sup>7</sup> These findings could have clinical implications for eyes with an already attenuated retinal vasculature, potentially exacerbating ischemic damage in eyes with DR. Although blocking VEGF decreases macular edema, it is important to investigate the effects of these treatments on the retinal microvasculature.<sup>8–12</sup>

Optical coherence tomography angiography (OCTA) is a noninvasive imaging method that has been used to study capillary changes in eyes with DR and to characterize the distinct macular capillary plexuses.<sup>13–15</sup> Interestingly, eyes with DME were shown to have lower vascular density in the deep capillary plexus (DCP) compared with non-DME eyes.<sup>16</sup> Although OCTA is widely used in DME, little attention has been paid to correcting OCTA artifacts such as suspended scattering particles in motion, which could lead to overestimations of DCP vessel density (VD).<sup>17</sup> In a study using swept-source OCTA, artifacts were found in approximately 25% of DME eyes.<sup>18</sup>

The purpose of this study was to use OCTA imaging to quantitatively characterize short-term retinal hemodynamic changes in patients with DME after a single intravitreal anti-VEGF injection. Given the various artifacts associated with DME, we also explored the most effective OCTA thresholding algorithm for the three capillary plexuses (superficial, middle, and deep retinal capillary plexuses). Different thresholding methods can yield significantly different quantitative OCTA results and can even impact the directionality of trends.<sup>19</sup> With the understanding that imaging artifacts in DME could potentially confound OCTA measurements, it is particularly important to identify the most effective thresholding algorithm. In this study, we demonstrate that the most reliable thresholding methods to remove background noise in DME depends on the capillary layer studied.

## Methods

### Study Sample

This prospective study was conducted in the Department of Ophthalmology at Northwestern University in

Chicago, Illinois, between April 2017 and October 2021 with approval from the Institutional Review Board of Northwestern University. This study was conducted in accordance with the Health Insurance Portability and Accountability Act regulations and the Declaration of Helsinki tenets. Individuals with DME treated with anti-VEGF injections, determined by review of electronic health records, were recruited from the clinic. All participants gave written informed consent before images were obtained.

Inclusion criteria were subjects with diabetes and eyes with center-involved DME based on OCT central subfield thickness of more than 240  $\mu\text{m}$ , the presence of residual cystic or intraretinal fluid requiring anti-VEGF treatment, and clinical assessment by board-certified ophthalmologists. Only eyes that had baseline OCTA scan before anti-VEGF injection and follow-up OCTA scan after anti-VEGF injection were included in the current study. Patients diagnosed with either type 1 or type 2 diabetes were included. Eyes with prior ocular interventions for diabetes (e.g., panretinal photocoagulation, surgery, or intravitreal injection) or nonvisually significant cataracts were not excluded from the study. Individuals with age-related macular degeneration were excluded from the study.

The International Clinical Diabetic Retinopathy Disease Severity Scale was used to classify patients with proliferative DR or nonproliferative DR (NPDR) as mild, moderate, or severe based on color fundus photographs.<sup>20</sup> In this staging system, patients with only microaneurysms are staged as mild NPDR, whereas patients with more than just microaneurysms such as soft exudates, venous beading, or hemorrhages or microaneurysms that do not meet severe NPDR criteria are staged as moderate NPDR. Severe NPDR was staged if there were four quadrants of hemorrhages or microaneurysms, two quadrants of venous beading, or one quadrant of intraretinal microvascular abnormalities exceeding standard reference photographs with no evidence of proliferative retinopathy.

Subjects with baseline imaging but without follow-up OCTA scans within 3 months from anti-VEGF injections were excluded. Follow-up OCTA scan was done at patients' next scheduled appointment in clinic. Additional study-specific appointments were scheduled for imaging patients who did not have a clinical visit within the study window. Eyes with motion artifact on OCTA scan or poor OCTA image quality, defined as quality index (Q-score) of less than 5 and a signal strength index (SSI) of less than 48 were also excluded.

Demographic and clinical information were reviewed and extracted from the electronic medical records.

## OCTA Imaging

Using the RTVue-XR Avanti System (Optovue, Inc., Fremont, CA) with split spectrum amplitude decorrelation angiography software (version 2017.1.0.151),  $3 \times 3 \text{ mm}^2$  OCTA scans centered on the fovea were acquired.<sup>21</sup> Specifications of the machine include A-scan rate of 70,000 scans per second and light source centered at 840 nm with a bandwidth of 45 nm. Two B-scans (M-B frames) were captured consecutively with each containing 304 A-scans. Split spectrum amplitude decorrelation angiography software was used for angiographic flow information generation. The SSI and quality index (Q-score) which represent the overall quality of image were obtained from the machine's proprietary software.

## Image Analysis Segmentation

Using default segmentation parameters, OCTA images of the full retinal angiogram and the superficial capillary plexus (SCP) were segmented using the built-in AngioVue Analytics software (version 2017.1.0.151). The full retinal thickness OCTA was segmented from the internal limiting membrane to 10  $\mu\text{m}$  below the outer plexiform layer. The SCP was segmented from the internal limiting membrane to 10  $\mu\text{m}$  above the inner plexiform layer (IPL). Manual segmentation was performed on the instrument to obtain the middle capillary plexus (MCP) and DCP, as described previously.<sup>22</sup> The MCP was segmented from 10  $\mu\text{m}$  above the IPL to 30  $\mu\text{m}$  below the IPL. The DCP was segmented from 30  $\mu\text{m}$  below the IPL to 10  $\mu\text{m}$  below the outer plexiform layer.

## Calculation of OCTA Parameters

OCTA parameters were obtained for the parafoveal region, defined as the annulus centered on the fovea with inner and outer ring diameters of 1 and 3 mm, respectively. All image analyses were performed using ImageJ (developed by Wayne Rasband, National Institutes of Health, Bethesda, MD; available at <http://rsb.info.nih.gov/ij/index.html>) by two separate graders. The central foveal thickness (CFT) was also obtained from the machine from the full retinal thickness scan.

The foveal avascular zone (FAZ) area was manually traced and calculated as previously described.<sup>22</sup> The adjusted flow index (AFI) is an indirect measure of blood flow based on the average pixel density of all vessels in the parafoveal region and was calculated according to previously described protocols via image J.<sup>23</sup> The parafoveal VD, calculated as the percentage

of pixels occupied by blood vessels in the parafoveal region, was obtained directly from the built-in machine software for the full retina, SCP, and MCP layers. The VD of the DCP layer was calculated according to previously described protocols.<sup>23</sup>

Each image was binarized and then skeletonized by the ImageJ open source plugin Skeletonize3D (developed by Ignacio Arganda-Carreras; available at <http://imagej.net/Skeletonize3D>) as shown in Figure 1.<sup>24</sup> Skeletonized images were used to determine the skeletonized VD, also known as vessel length density (VLD), which represents all vessels skeletonized to 1 pixel width. This function eliminates the influence of larger arterioles and venules on density measurements in contrast with the VD, which will disproportionately represent larger arterioles and venules.

## Binarization and Thresholding Validation Methods

Because thresholding methods may impact the measured parameters, we compared two different thresholding methods to identify the method that more accurately represents the ground truth in the different capillary layers.<sup>23</sup> In the previously reported VLD-based thresholding method for the DCP,<sup>23</sup> a custom ImageJ macro was used to calculate DCP skeletonized VLD for a variety of possible threshold values. These calculated VLDs were then plotted against the threshold values on a graph. Because noise presumably decreases faster than the true vessel signal, the optimal threshold value is determined to be the point where the DCP vessel length versus threshold curve transitions from steep to shallow. Best fit lines were drawn on the DCP VLD versus threshold plot (Fig. 2). The intersection of these the two lines was calculated and represents the DCP binarization threshold that we used. This approach allowed us to better distinguish the true vessel signal from noise by using an individualized threshold for each eye.<sup>23</sup>

To validate the thresholding method, we prospectively performed five repeated OCTA scans on nine eyes with DME. In these eyes, we performed image segmentation, registration, and averaging to generate an averaged scan for the full retina as well as the SCP, MCP, and DCP slabs. Using the averaged scans, we calculated the ground truth parafoveal VD using an automated method (Huang) available in ImageJ (Fig. 3a).<sup>23</sup> The VD from the proprietary software and VLD-based methods were then compared with the ground truth VD for each layer (Fig. 3b).<sup>23</sup> We compared the mean absolute error between the ground truth VD for

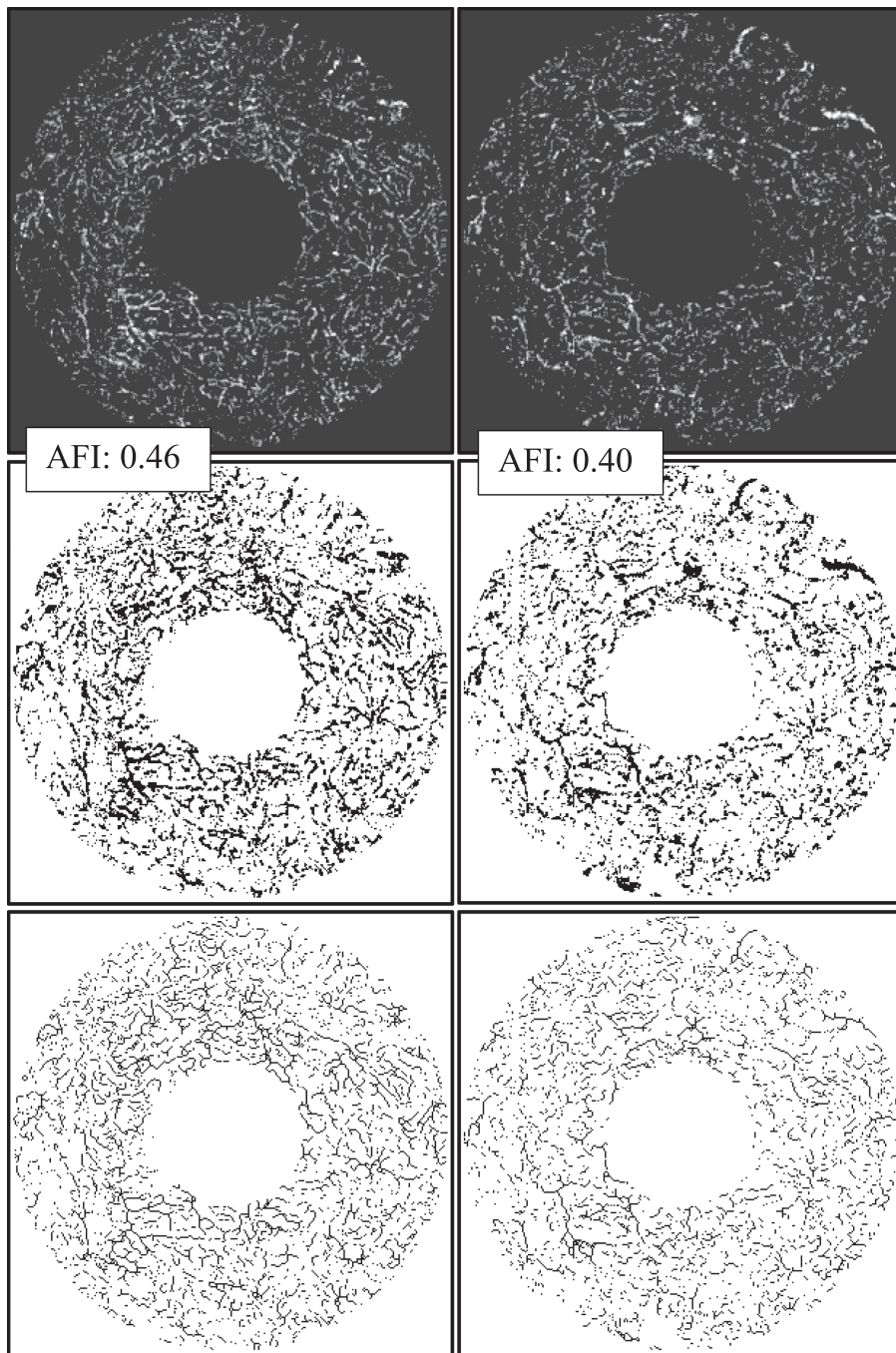


**Figure 1.** Optical OCTA of the DCP from baseline to follow-up with AFI. (*Top row*) Parafoveal area of DCP at baseline (*left*) and follow-up (*right*). (*Middle row*) Binarized parafoveal area of DCP at baseline (*left*) and follow-up (*right*). (*Bottom row*) Skeletonized parafoveal area of DCP at baseline (*left*) and follow-up (*right*).

each layer to the other two methods using a two-sided paired *t* test.

Based on these results, we used the threshold from the VLD-based method for subsequent calculations of the DCP layer.<sup>23</sup> The VD of the full retina, SCP, and the MCP layers were based on the proprietary

software. However, because this proprietary software did not provide the AFI values, we used the FAZ signal on a full-thickness angiogram to find the threshold for subsequent manual image analyses, as previously described.<sup>22,24,25</sup> This threshold was then used to calculate the AFI and VLD of the SCP.

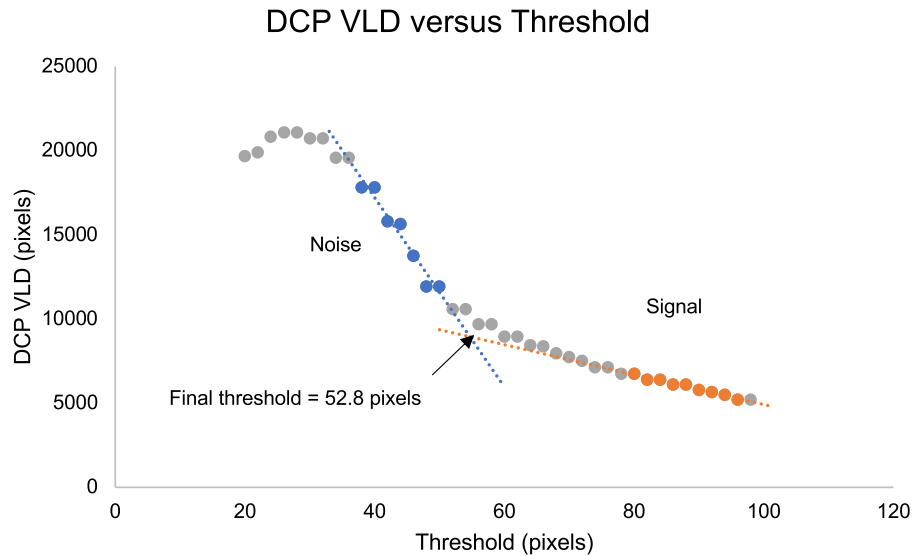


**Figure 2.** Example of DCP VLD-based thresholding method. For a variety of possible threshold values, the DCP VLD is calculated and plotted on a graph. Two regression lines are fitted, with one on the steep region of the curve representing noise (blue) and one on the plateau region of the curve representing signal (orange). The final chosen threshold for this particular image is located at the intersection of the regression lines (black arrow).

## Statistical Analyses

Statistical analyses were performed with SPSS version 28 (IBM SPSS Statistics; IBM Corporation, Chicago, IL). Statistical significance was defined as a  $P$  value of less than 0.05. Two-way mixed intraclass correlation coefficient (ICC) was used to assess intergrader reliability for threshold measurements gathered from full retinal scan and DCP scans. Pearson correlations were used to evaluate associations between potential confounding variables and OCTA parameters. Shapiro–Wilk tests were performed to determine normal distribution of OCTA parameter data. A generalized linear model with a repeated measures design was used for comparing OCTA parameters comparison between baseline and follow-up scans.

## Results

### Demographics

We included a total of 26 eyes of 22 patients (aged  $60.2 \pm 13.7$  years) who had prospective OCTA scan before and after anti-VEGF injection for DME (mean interval between OCTA,  $31.1 \pm 17.3$  days). Overall patient demographic and clinical characteristics are summarized in Table 1. All eyes had center involving DME requiring anti-VEGF treatment.

## Evaluation of Thresholding Methods

For the DCP layer, the mean absolute error of the VLD-based method was smaller than that of the AngioVue output ( $P = 0.042$ ). For the SCP layer, the opposite was true ( $P = 0.037$ ). For the full retina and MCP layer, the AngioVue method had a smaller mean absolute error than the VLD-based method, but the difference between the two methods was not statistically significant ( $P = 0.46$  and  $P = 0.42$ , respectively, for these two slabs) (Figs. 2c, d).

Overall, based on this analysis, we found that, for DME eyes, the VLD-based method is significantly more accurate for the DCP slab, the proprietary software output is more accurate for the SCP layer, and the two methods performing similarly for the full retina and MCP slabs. Therefore, for subsequent image analysis, when calculating the VD, we used the VLD-based method for the DCP slab and the software output for the VD in the MCP, SCP, and full retina layers.

## Comparison of OCTA Parameters Between Baseline and Follow-up

Threshold measurements used for AFI and VLD calculations by the two separate graders had an ICC of 0.990 (95% confidence interval [CI], 0.971–0.996) for the full retinal layer, SCP, and MCP and an ICC of 0.991 (95% CI, 0.974–0.997) for the DCP. FAZ

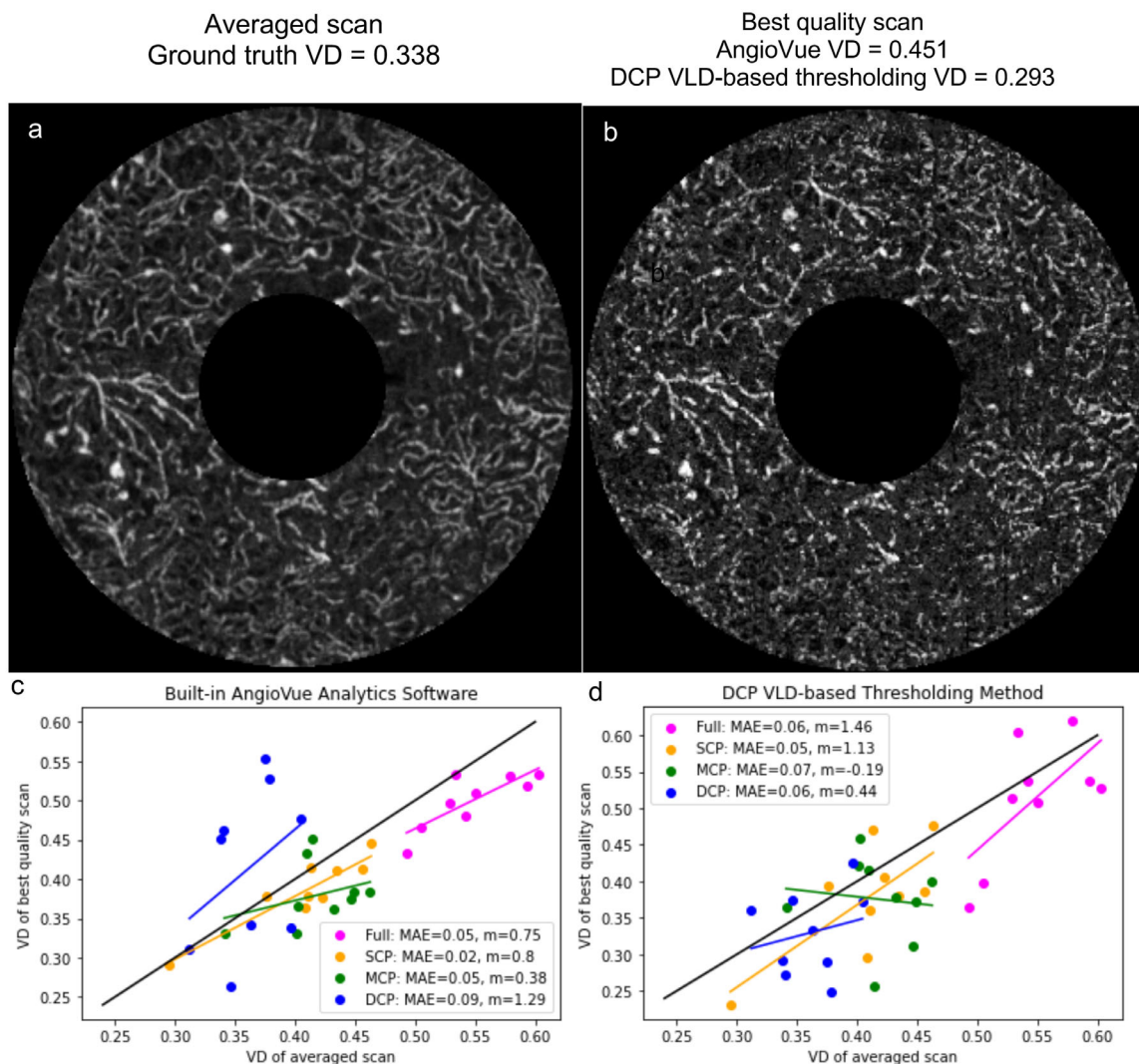


**Figure 3.** Evaluating Different OCTA Thresholding Methods for DME Eyes. (a) Example of an averaged scan of the DCP layer in a DME eye. (b) Best quality scan out of the 5 scan used to generate the average image in with black line indicating ideal fit line (a). Here, the VLD-based method (VD = 0.293) matches the ground truth VD (VD = 0.338) more closely than the AngioVue method (VD = 0.451). (c, d) Graph comparing the AngioVue method (c) and the VLD- based method (d) with the averaged scan VD. MAE, mean absolute error; m, slope of the best fit line.

measurements by the two separate graders had an ICC of 0.991 (95% CI, 0.975–0.997).

The SSI and Q-scores, which are proxies for image quality, were compared using paired *t* tests and found to be not significantly different between baseline OCTA scans from follow-up scans. The CFT ( $P = .003$ ) was found to be significantly decreased comparing baseline with follow-up, consistent with prior studies.<sup>26</sup> Pearson correlation coefficient analysis indicated SSI and Q-score showed significant associations with OCTA parameters along with baseline CFT (Supplementary Table S1). Therefore, we chose to adjust for Q-score

along with CFT in the subsequent OCTA outcome analysis.

We found the DCP AFI was significantly decreased on follow-up OCTA scans ( $P = 0.010$ ) compared with baseline. We also found significant decreases in FAZ area ( $P < 0.001$ ) via generalized linear model and significant decreases in CFT ( $P = 0.003$ ) from baseline via paired *t* tests. Detailed findings are summarized in Table 2.

No significant differences were found for VD in any layer or VLD of the SCP comparing the baseline OCTA scan compared with the follow-up scans.

**Table 1.** Demographic and Clinical Characteristics of Study Patients

Patients	22
Eyes	26
Age, years	60.2 ± 13.7
Sex	
Female	11 (50)
Male	11 (50)
Diabetes	
Type 1	4 (18)
Type 2	18 (82)
Disease duration, years	19.0 ± 11.3
DR Dx	
Mild NPDR	3 (12)
Moderate NPDR	10 (38)
Severe NPDR	3 (12)
PDR	10 (38)
PRP treated	8 (80)
No PRP	2 (20)
Last HbA1c	7.6 ± 1.4
Mean Interval between OCTA scans (days)	31.1 ± 17.3
Treatment	
Naïve	3 (12)
Previous treatment (e.g., intravitreal injections, panretinal photocoagulation)	23 (88)
Prior intravitreal injections	
<10	17 (65)
10–19	2 (8)
20–29	2 (8)
≥30	5 (19)

Values are number, number (%), or mean ± standard deviation.

Overall, the AFI trends were similar in all layers except for the MCP *P* Value < 0.05.

## Discussion

In this study, we used OCTA to study retinal hemodynamic changes in the retinal capillaries after an anti-VEGF injection in eyes with DME. Using the OCTA parameter of AFI, which serves as a proxy for blood flow, we found a significant decrease in AFI of the DCP layer after anti-VEGF injection. We also performed a systematic analysis of the different thresholding approaches to identify the most accurate approach for the three capillary plexuses in eyes with DME. We found that the VLD-based method is significantly more accurate for the DCP slab, whereas the

proprietary software output was acceptable for the full, MCP, and SCP layer.<sup>18,23</sup> This finding will be useful for researchers using OCTA in eyes with DME.

The most salient finding in our study was that the AFI was significantly decreased in the DCP layer, which suggests a disruption of deep retinal perfusion after a single anti-VEGF injection in eyes with DME. In contrast, using fluorescein angiography (FA), large randomized controlled clinical trials found no worsening of macular perfusion after following anti-VEGF in eyes with DME.<sup>27</sup> This finding is not surprising; the DCP is not visualized by FA and can only be discerned using the depth resolved OCTA scans.<sup>28,29</sup> Furthermore, OCTA has unique advantages over FA and, being unperturbed by leakage, is generally much better at resolving capillary nonperfusion.<sup>30</sup> Our AFI results suggest perfusion-related injury to ocular structures cannot be ruled out in patients receiving intravitreal injections. Unlike previous studies, we used the VLD-based threshold for the DCP based on our systematic analysis. Our study was uniquely positioned to investigate hemodynamic responses in previously treated individuals, a population that is clinically relevant. This would fit with the patient population most impacted by hemodynamic disruptions that could potentially exacerbate their preexisting ischemia. Because retinal microvascular impairment in the DCP correlates with DME severity, further disruption of retinal perfusion during anti-VEGF therapy could be detrimental to this specific capillary plexus.<sup>31</sup>

Decreased CFT is consistent with reduced DME after anti-VEGF intravitreal injections, as would be expected. Several studies using FA images have reported enlargement of the FAZ after anti-VEGF therapy, which could be related to decreased leakage and better definition of the FAZ boundaries.<sup>32,33</sup> Ghasemi Falavarjani et al.<sup>34</sup> examined the SCP and DCP FAZ separately on OCTA and did not find significant differences after anti-VEGF therapy in eyes with DME or secondary to retinal vein occlusion. Different from this latter study, we measured the FAZ area of the full retinal slab rather than the separate capillary plexuses. Separating the FAZ into different vascular plexuses may increase variability, whereas a single full retina FAZ may provide more accurate measurements.<sup>35–38</sup> Displacement of vessels owing to edema could also displace the FAZ border laterally. A decrease in edema would be consistent with a corresponding decrease in FAZ area in the full retinal slab, as we have found. Thus, measurement of a single FAZ in the full retinal slab allowed us to capture these global changes.

Previous studies have not explored the accuracy of OCTA thresholding methods in eyes with DME. In one study analyzing averaged OCTA scans, images

**Table 2.** OCTA Retinal Hemodynamic Imaging Outcomes at Baseline Versus Follow-Up

Measurement (Mean $\pm$ SD)	Baseline Mean (n = 26)	Follow-Up Mean (n = 26)	P Value
SSI	58.65 $\pm$ 6.34	59.58 $\pm$ 7.22	0.373
Q-Score	7.15 $\pm$ 1.05	7.12 $\pm$ 1.07	0.840
CFT	339.53 $\pm$ 75.86	314.92 $\pm$ 69.96	<b>0.003</b>
FAZ	0.3362 $\pm$ 0.1598	0.3173 $\pm$ 0.1492	<b>&lt;0.001</b>
AFI			
Full Retina	0.441 $\pm$ 0.058	0.439 $\pm$ 0.062	0.639
SCP	0.452 $\pm$ 0.057	0.450 $\pm$ 0.060	0.742
MCP	0.424 $\pm$ 0.064	0.428 $\pm$ 0.069	0.248
DCP	0.430 $\pm$ 0.023	0.417 $\pm$ 0.043	<b>0.010</b>
VD			
Full retina	46.185 $\pm$ 6.771	46.877 $\pm$ 5.770	0.201
SCP	37.065 $\pm$ 6.127	36.881 $\pm$ 5.856	0.467
MCP	41.085 $\pm$ 5.636	41.246 $\pm$ 6.084	0.844
DCP	25.423 $\pm$ 6.330	27.253 $\pm$ 7.087	0.093
VLD			
SCP	13.046 $\pm$ 2.894	13.344 $\pm$ 2.948	0.984

Imaging characteristics (SSI, Q-score, CFT) were compared using paired *t* tests. OCTA measurements (FAZ, AFI, VD, and VLD) were compared using generalized linear model adjusted for CFT and Q-score. Values presented in bold are significant as defined by *p*-value < 0.05.

were binarized using the autothresholding function on ImageJ to measure the VD.<sup>39</sup> Other OCTA studies have used the built-in software values for VD.<sup>26,34</sup> However, it is important to critically assess the threshold choice for binarization because it significantly impacts quantitative measurements, including VD and VLD.<sup>19</sup> By comparing the two methods with ground-truth values (VD data extracted from averaged OCTA scans), we found that the VLD-based thresholding is more accurate for the DCP slab, whereas the built-in method more accurately reproduces the ground truth VD for the SCP layer, and performed similarly to the VLD-based thresholding method for the MCP and full retina layers.<sup>23</sup> In particular, our use of the VLD thresholding method for the DCP slab allowed us to be confident of our results in that layer.

We found no significant changes in the VD or VLD in any of the capillary layers. Other studies that examined these parameters have yielded variable results. Most studies did not find significant differences, consistent with our study.<sup>26</sup> Previously, a retrospective longitudinal study using OCTA has reported significantly increased VD after anti-VEGF treatment for DME, different from our study findings.<sup>40</sup> This finding was attributed to response to treatment as eyes with DME had a lower VD at baseline as compared with healthy eyes and a decreased VD was correlated with worsening DR.<sup>40</sup> A small subset of studies found

a significantly decreased VD in the SCP after injections in macular edema secondary to retinal vein occlusion.<sup>34,41</sup> OCTA capillary segmentation could possibly account for the differences, because these studies did not consider the MCP.<sup>34,40,41</sup> By segmenting the three capillary plexuses, we achieved better specificity of sublayer VD. Because we evaluated these metrics in the short term (after one injection), we cannot exclude the possibility of chronic, progressive changes that may be more obvious on longer follow-up.

Our study was limited by its small sample size, which was imposed by our strict quality and inclusion criteria. Different anti-VEGF agents may have distinct effects on the capillaries, but our small sample did not allow us to adjust for this factor. Furthermore, previous injection history was not an exclusion criterion for this study. And, although we did not find a correlation between vessel parameters and total number of injections, our cross-sectional dataset along with the small sample does not allow us to resolve the possible cumulative impact of chronic therapy. We considered the possibility that edema and microaneurysms at baseline in DME eyes could potentially induce shadow artifacts and artifactual ischemia. We would expect that, with treatment, the resolution of these findings would remove the artifactual ischemia. With that, we would anticipate an artifactually increased flow after injection. Our findings of decreased flow after

injections are in the opposite direction, which reassures us that these types of artifacts, even if they were present at baseline, did not have a prominent effect on our results. In fact, it is more likely that these artifacts are attenuating the magnitude of our main outcome metric.

## Conclusions

Our finding of decreased AFI in the DCP layer suggests decreased deep retinal perfusion after a single anti-VEGF injection in eyes with DME. Additional prospective research is needed to explore these findings with long-term anti-VEGF use as well as explore the interaction between baseline macular ischemia and the injections. We have validated the VLD thresholding as most effective for the DCP in eyes with DME.<sup>23</sup> Additional large prospective trials using OCTA are necessary to confirm our results.

## Acknowledgments

Funded in part by NIH grant R01 EY31815 (AAF). Instrument support was provided by Optovue, Inc., Fremont, California. All funders had no role in study design, data collection and analysis, publication decision, or manuscript preparation.

Disclosure: **J. Song**, None; **B.B. Huang**, None; **J.X. Ong**, None; **N. Konopek**, None; **A.A. Fawzi**, None

## References

1. Browning DJ, Stewart MW, Lee C. Diabetic macular edema: evidence-based management. *Indian J Ophthalmol*. 2018;66(12):1736–1750.
2. Grant MB, Afzal A, Spoerri P, Pan H, Shaw LC, Mames RN. The role of growth factors in the pathogenesis of diabetic retinopathy. *Expert Opin Investig Drugs*. 2004;13(10):1275–1293.
3. Shimura M, Kitano S, Muramatsu D, et al. Real-world management of treatment-naïve diabetic macular oedema in Japan: two-year visual outcomes with and without anti-VEGF therapy in the STREAT-DME study. *Br J Ophthalmol*. 2020;104(9):1209–1215.
4. Osaadon P, Fagan XJ, Lifshitz T, Levy J. A review of anti-VEGF agents for proliferative diabetic retinopathy. *Eye (Lond)*. 2014;28(5):510–520.
5. Papadopoulou DN, Mendrinou E, Mangioris G, Donati G, Pournaras CJ. Intravitreal ranibizumab may induce retinal arteriolar vasoconstriction in patients with neovascular age-related macular degeneration. *Ophthalmology*. 2009;116(9):1755–1761.
6. Sacu S, Pemp B, Weigert G, et al. Response of retinal vessels and retrobulbar hemodynamics to intravitreal anti-VEGF treatment in eyes with branch retinal vein occlusion. *Invest Ophthalmol Vis Sci*. 2011;52(6):3046–3050.
7. Mendrinou E, Mangioris G, Papadopoulou DN, Donati G, Pournaras CJ. Long-term results of the effect of intravitreal ranibizumab on the retinal arteriolar diameter in patients with neovascular age-related macular degeneration. *Acta Ophthalmol*. 2013;91(3):e184–e190.
8. Massin P, Bandello F, Garweg JG, et al. Safety and efficacy of ranibizumab in diabetic macular edema (RESOLVE Study): a 12-month, randomized, controlled, double-masked, multicenter phase II study. *Diabetes Care*. 2010;33(11):2399–2405.
9. Nishijima K, Ng YS, Zhong L, et al. Vascular endothelial growth factor-A is a survival factor for retinal neurons and a critical neuroprotectant during the adaptive response to ischemic injury. *Am J Pathol*. 2007;171(1):53–67.
10. Campochiaro PA, Wyckoff CC, Shapiro H, Rubio RG, Ehrlich JS. Neutralization of vascular endothelial growth factor slows progression of retinal nonperfusion in patients with diabetic macular edema. *Ophthalmology*. 2014;121(9):1783–1789.
11. Nguyen QD, Brown DM, Marcus DM, et al. Ranibizumab for diabetic macular edema: results from 2 phase III randomized trials: RISE and RIDE. *Ophthalmology*. 2012;119(4):789–801.
12. Wells JA, Glassman AR, Ayala AR, et al. Aflibercept, bevacizumab, or ranibizumab for diabetic macular edema: two-year results from a comparative effectiveness randomized clinical trial. *Ophthalmology*. 2016;123(6):1351–1359.
13. Durbin MK, An L, Shemonski ND, et al. Quantification of retinal microvascular density in optical coherence tomographic angiography images in diabetic retinopathy. *JAMA Ophthalmol*. 2017;135(4):370–376.
14. Nesper PL, Roberts PK, Onishi AC, et al. Quantifying microvascular abnormalities with increasing severity of diabetic retinopathy using optical coherence tomography angiography. *Invest Ophthalmol Vis Sci*. 2017;58(6):BIO307–BIO315.
15. Onishi AC, Nesper PL, Roberts PK, et al. Importance of considering the middle capillary

- plexus on OCT angiography in diabetic retinopathy. *Invest Ophthalmol Vis Sci.* 2018;59(5):2167–2176.
16. Lee J, Moon BG, Cho AR, Yoon YH. Optical coherence tomography angiography of DME and its association with anti-VEGF treatment response. *Ophthalmology.* 2016;123(11):2368–2375.
  17. Maltsev DS, Kulikov AN, Kazak AA, Freund KB. Suspended scattering particles in motion may influence optical coherence tomography angiography vessel density metrics in eyes with diabetic macular edema. *Retina.* 2021;41(6):1259–1264.
  18. Podkowinski D, Beka S, Mursch-Edlmayr AS, Strauss RW, Fischer L, Bolz M. A swept source optical coherence tomography angiography study: imaging artifacts and comparison of non-perfusion areas with fluorescein angiography in diabetic macular edema. *PLoS One.* 2021;16(4):e0249918.
  19. Mehta N, Liu K, Alibhai AY, et al. Impact of binarization thresholding and brightness/contrast adjustment methodology on optical coherence tomography angiography image quantification. *Am J Ophthalmol.* 2019;205:54–65.
  20. Wilkinson CP, Ferris FL, 3rd, Klein RE, et al. Proposed international clinical diabetic retinopathy and diabetic macular edema disease severity scales. *Ophthalmology.* 2003;110(9):1677–1682.
  21. Jia Y, Tan O, Tokayer J, et al. Split-spectrum amplitude-decorrelation angiography with optical coherence tomography. *Opt Express.* 2012;20(4):4710–4725.
  22. Nesper PL, Lee HE, Fayed AE, Schwartz GW, Yu F, Fawzi AA. Hemodynamic response of the three macular capillary plexuses in dark adaptation and flicker stimulation using optical coherence tomography angiography. *Invest Ophthalmol Vis Sci.* 2019;60(2):694–703.
  23. Ong JX, Kwan CC, Cicinelli MV, Fawzi AA. Superficial capillary perfusion on optical coherence tomography angiography differentiates moderate and severe nonproliferative diabetic retinopathy. *PLoS One.* 2020;15(10):e0240064.
  24. Chu Z, Lin J, Gao C, et al. Quantitative assessment of the retinal microvasculature using optical coherence tomography angiography. *J Biomed Opt.* 2016;21(6):66008.
  25. Ashraf M, Nesper PL, Jampol LM, Yu F, Fawzi AA. Statistical model of optical coherence tomography angiography parameters that correlate with severity of diabetic retinopathy. *Invest Ophthalmol Vis Sci.* 2018;59(10):4292–4298.
  26. Sellam A, Glacet-Bernard A, Coscas F, Miere A, Coscas G, Souied EH. Qualitative and quantitative follow-up using optical coherence tomography angiography of retinal vein occlusion treated with anti-VEGF: optical coherence tomography angiography follow-up of retinal vein occlusion. *Retina.* 2017;37(6):1176–1184.
  27. Wykoff CC, Shah C, Dhoot D, et al. Longitudinal retinal perfusion status in eyes with diabetic macular edema receiving intravitreal aflibercept or laser in VISTA Study. *Ophthalmology.* 2019;126(8):1171–1180.
  28. Spaide RF, Klancnik JM, Jr., Cooney MJ. Retinal vascular layers imaged by fluorescein angiography and optical coherence tomography angiography. *JAMA Ophthalmol.* 2015;133(1):45–50.
  29. Ong JX, Fawzi AA. Perspectives on diabetic retinopathy from advanced retinal vascular imaging. *Eye (Lond).* 2022;36(2):319–327.
  30. Couturier A, Mane V, Bonnin S, et al. Capillary plexus anomalies in diabetic retinopathy on optical coherence tomography angiography. *Retina.* 2015;35(11):2384–2391.
  31. Agemy SA, Scripsema NK, Shah CM, et al. Retinal vascular perfusion density mapping using optical coherence tomography angiography in normals and diabetic retinopathy patients. *Retina.* 2015;35(11):2353–2363.
  32. Neubauer AS, Kook D, Haritoglou C, et al. Bevacizumab and retinal ischemia. *Ophthalmology.* 2007;114(11):2096.
  33. Sim DA, Keane PA, Zarranz-Ventura J, et al. Predictive factors for the progression of diabetic macular ischemia. *Am J Ophthalmol.* 2013;156(4):684–692.
  34. Ghasemi Falavarjani K, Iafe NA, Hubschman JP, Tsui I, Sadda SR, Sarraf D. Optical coherence tomography angiography analysis of the foveal avascular zone and macular vessel density after anti-VEGF Therapy in eyes with diabetic macular edema and retinal vein occlusion. *Invest Ophthalmol Vis Sci.* 2017;58(1):30–34.
  35. Campbell JP, Zhang M, Hwang TS, et al. Detailed vascular anatomy of the human retina by projection-resolved optical coherence tomography angiography. *Sci Rep.* 2017;7:42201.
  36. Nesper PL, Fawzi AA. Human parafoveal capillary vascular anatomy and connectivity revealed by optical coherence tomography angiography. *Invest Ophthalmol Vis Sci.* 2018;59(10):3858–3867.
  37. Park JJ, Soetikno BT, Fawzi AA. Characterization of the middle capillary plexus using optical coherence tomography angiography in healthy and diabetic eyes. *Retina.* 2016;36(11):2039–2050.
  38. Hwang TS, Zhang M, Bhavsar K, et al. Visualization of 3 distinct retinal plexuses by

- projection-resolved optical coherence tomography angiography in diabetic retinopathy. *JAMA Ophthalmol.* 2016;134(12):1411–1419.
39. Le Boite H, Chetrit M, Erginay A, et al. Impact of image averaging on vessel detection using optical coherence tomography angiography in eyes with macular oedema and in healthy eyes. *PLoS One.* 2021;16(10):e0257859.
40. Hsieh YT, Alam MN, Le D, et al. OCT angiography biomarkers for predicting visual outcomes after ranibizumab treatment for diabetic macular edema. *Ophthalmol Retina.* 2019;3(10):826–834.
41. Barash A, Chui TYP, Garcia P, Rosen RB. Acute macular and peripapillary angiographic changes with intravitreal injections. *Retina.* 2020;40(4):648–656.